Technoeconomic Insights into Metal Hydrides for Stationary Hydrogen Storage

Xinyi Wang[1,2], Peng Peng[1], Matthew D. Witman[3], Vitalie Stavila[3], Mark D. Allendorf[3], Hanna M. Breunig[1*]

[1]Lawrence Berkeley National Laboratory, Berkeley, CA 94720, United States

[2] Department of Mechanical Engineering, California State University, Fullerton, Fullerton, CA 92870, United States

[3] Sandia National Laboratories, Livermore, CA 94550, United States

*Corresponding author: hannabreunig@lbl.gov

Abstract

Metal hydrides (MHs) are promising candidates for hydrogen storage due to their high volumetric energy densities and safety features. Recent developments suggest hydride systems can cycle and operate at pressures and temperatures favorable coupling with fuel cells for stationary long-duration energy storage applications. In this study, we present a conceptual design of a metal hydride-based storage system for backup power (0 to 20 MW supplied over 0 to 100 hours), and benchmark system cost and performance. Leveraging experimental hydrogen absorption and desorption data, we determine the uptake/release of hydrogen across likely pressure and temperature conditions, and estimate the equipment power, upfront capital cost, levelized cost of storage, land footprint, and energy density for a select number of metal hydrides and hypothetical operation scenarios. Our findings indicate that hydride-based storage systems hold significant size advantage in physical footprint, requiring up to 65% less land than the 170-bar compressed gas storage options. Metal hydride systems can be cost competitive with 350-bar compressed gas systems, with $TiFe_{0.85}Mn_{0.05}$ achieving \$0.453/kWh and complex MH $2Mg(NH_2)_2$-2.1LiH-0.1KH achieving \$0.383/kWh, compared to \$0.397/kWh for 350 bar compressed gas in the base case scenario. However, these advantages are sensitive to charging and discharging rate requirements, operational cycles and material manufacturing prices. Extending charging times and increasing operating cycles significantly reduce LCOS, especially for complex MHs, making them more competitive for applications with slow charging and long duration energy storage needs. Key strategies to further enhance the competitiveness of MHs include leveraging waste heat from fuel cells, increasing hydrogen uptake, and achieving metal hydride production costs of US\$10/kg.

Keywords: Hydrogen storage, energy storage, backup power, metal hydride, techno-economic analysis

Introduction

Ensuring a reliable power supply is essential for modern society. Power outages cost American businesses around $150 billion annually, according to the U.S. Department of Energy[1]. The increasing frequency and severity of these outages, driven by climate change, make reliable power even more critical[2]. This is particularly true for essential infrastructures, such as health care and data centers, where extended outages can disrupt medical operations, endanger public health, and lead to substantial data loss and security breaches. To address these challenges and ensure a dependable energy supply, these facilities often rely on diesel or natural gas generators as backup power[3–5].

Hydrogen powered fuel cells are emerging as a highly promising low-carbon alternative to diesel backup power generators, particularly when paired with on-site production of hydrogen using renewable energy[6]. There are many ongoing research efforts focusing on developing hydrogen fuel cell backup power systems in critical infrastructure applications[7–9]. However, a significant challenge that needs to be addressed is the requirement of long duration storage of energy or hydrogen[10–13]. Due to its low volumetric energy density, for backup power, hydrogen storage systems are being proposed that rely on compression (170 bar to 350 bar) or cooling and liquefaction (-253°C). Such systems are costly, and presently challenged by hydrogen leakage and safety concerns[14–17]. As an alternative storage technology, metal hydrides (MHs) can reversibly store hydrogen in a solid state under moderate storage conditions[18]. For large scale hydrogen storage applications, such as backup power, MHs that store hydrogen at lower pressures offer a safer and more efficient alternative to high-pressure compressed gas. They provide stable, long-term storage with reduced risk of leakage [19,20].

Intermetallic and complex MHs are among the most studied materials for reversible hydrogen storage applications[15]. Intermetallic hydrides are formed by combining hydrogen atoms with intermetallic compounds composed of two or more metals. The principle behind intermetallic hydrides is that an alloy $A_xB_yH_z$, containing one element (A) that binds hydrogen strongly and another (B) that binds it weakly, can exhibit hydrogen storage properties intermediate to those of its constituent elements[17,21]. In practice, a limited number of intermetallic hydride structures, such as those with AB, AB_2 or AB_5 crystal structures, are commonly proposed for hydrogen storage applications[22]. Complex MHs store hydrogen in a complex anion form bonded to a metallic cation,

offering high hydrogen storage capacity[17]. Despite their high volumetric energy density, recent system-level performance of MH-based hydrogen storage have primarily focused on transportation applications[16,23–28]. Although there has been recent progress in developing these materials for stationary long-duration energy storage applications, there is a notable lack of benchmarking key material-level and system-level stationary storage performance targets for comparison with incumbent systems such as compressed gas storage.

In this study, we present novel process designs for metal hydride-based hydrogen storage systems used in backup power applications (0 to 20 MW) and demonstrate targets for materials development. Our base case assumes a 10 MW 96-hour scale backup power system, representing the power and energy necessary to support critical infrastructure such as hospitals or data centers[29]. We adapt and employ a techno-economic analysis (TEA) approach for material screening and system evaluation developed previously for metal organic framework storage materials[30], in order to benchmark promising candidate hydrides with adequate experimental absorption/desorption data. From this data we calculate hydrogen uptake under various pressure and temperature conditions in the tank and determine the tank size and balance of plant designs to supply necessary heating, compression, and cooling. The results are benchmarked against 170- and 350-bar compressed gas storage operating under the same end user cycling scenarios. Finally, we discuss research gaps and offer a roadmap for material and system research that can further improve viability of this critical infrastructure advancement.

Methods

Back-up power system and operation cycles

In our base case, we model metal hydride hydrogen storage systems coupled with co-located electrolyzers and fuel cells sized to meet 10 MW backup power events lasting 96 hours[29]. In other words, the system can supply 10 MW power for 96 hours without recharging. The power scale, discharge duration, hydrogen release efficiency and fuel cell efficiency determine the total hydrogen storage requirement, with larger power scales or longer discharge durations necessitating greater hydrogen storage capacity. For the base case, charging time is set to 96 hours. We also analyze the effects of varying charging rates, including both fast and slow charging scenarios, which will be discussed later. Figure 1a illustrates the base case process flow of a metal hydride-

based hydrogen storage backup energy system. In this on-site stationary hydrogen backup system, hydrogen is generated by alkaline water electrolyzer stacks and stored in metal hydride-packed storage tanks. The storage system also includes ancillary facilities to manage cooling, compression, and heating requirements during the charge and discharge cycles. Hydrogen is reconverted to electricity via proton-exchanger membrane fuel cell stacks when needed. The operational cycle of the storage system is shown in Figure 1d. Initially, the storage tanks are assumed to be at room temperature. During the initial charging stage, the tanks are heated to the requisite temperature, and hydrogen from the electrolyzer is compressed and passed into the tanks to reach stage (2). During this phase, cooling of the gas and tanks is facilitated by coolants. After hydrogen absorption, the tanks are sealed, allowing the system to cool to room temperature, thereby storing hydrogen for extended periods. This design decision is based upon a cost comparison of ambient storage with reheating versus warm storage with thermal insulation. We calculate the costs of these two approaches: the first one is a stand-by mode, where after the charging, the system is allowed to cool to room temperature. When hydrogen needs to be discharged, the tank is reheated to the required operating temperature. The second approach involves maintaining the tank at a consistent temperature between the charging and discharging processes through continuous heating and insulation. The cost for these two methods is shown in Figure S6 As the number of charging and discharging cycles increases, the time between these processes shortens, reducing the energy cost required to maintain a constant temperature. However, the cost for the standby mode increases due to the need for more frequent reheating. Despite this, the standby mode still proves to be less expensive over the full cycle span, which is why we select it for further analysis. During periods of hydrogen demand, the storage system is reheated to the same temperature, releasing hydrogen from the tanks to the fuel cell stacks at 2 bar, reaching stage (3). Some hydrogen remains in the tank due to the release efficiency of the hydride materials. During this release, heat is supplied to maintain the temperature necessary for hydrogen desorption (ΔH_{des}). Following each discharge process, hydrogen for the next cycle is immediately recharged to the initial stage (1) as shown in Figure 1c. In the base case scenario, we assume 12 charge and discharge cycles per year, corresponding to 1152 hours of annual power outage. The impact of the number of cycles is investigated and will be discussed in the results. A higher number of cycles implies more frequent use of the storage system, which could potentially reduce the system's levelized cost of storage.

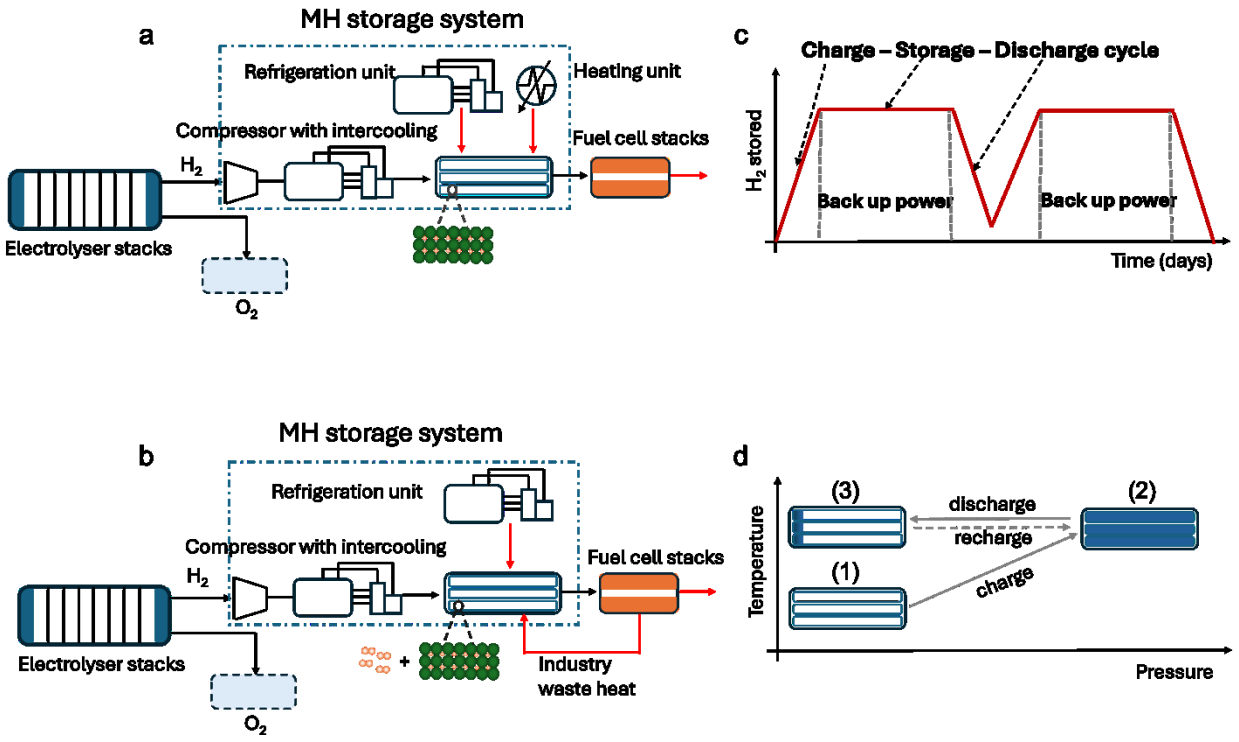

Figure 1. (a) Process flow for the base case scenario of a MH-based hydrogen storage back-up energy system, with main unit operations and system boundaries indicated by the dashed box. (b) Process flow for the alternative scenario featuring both gas phase hydrogen and metal hydride hydrogen storage; here, gas phase hydrogen initiates the fuel cell operation, which in turn provides the waste heat required for the hydrogen desorption from the metal hydride. (c) Schematic diagram illustrating the system cycles for charging, storing, discharging and recharging. (d) Overview of the temperature and pressure conditions across various stages.

Additionally, we developed a process flow for an alternative scenario as shown in Figure 1b where there is more gas-phase hydrogen in the storage tank. For certain intermetallic hydrides, if the operating temperature remains below 80 °C, the heat from the fuel cell coolant is sufficient to facilitate hydrogen desorption and reduce operational costs[31]. In this setup, we oversize the storage tanks to allow for 5 wt% gas phase hydrogen alongside hydrides in the storage tanks. The gas phase hydrogen is released first to activate the fuel cells, whose waste heat, conveyed by a coolant fluid, is then utilized to heat the metal hydride storage system for hydrogen desorption.

Material selection and storage tank models

We select representative MHs and take experimental pressure-composition-temperature (PCT) curves from the literature for AB (TiFe and $TiFe_{0.85}Mn_{0.05}$)[32], AB2 ($Ti_{0.95}Zr_{0.05}Mn_{1.55}V_{0.45}Fe_{0.09}$)[33], AB5 ($MnNi_{4.6}Fe_{0.4}$)[33] intermetallic hydrides and complex MH ($2Mg(NH_2)_2$-2.1LiH-0.1KH)[25,34]. Intermetallic hydrides are based on an alloy composition, $A_xB_yH_z$, where the element(s) in A and B respectively bind hydrogen strongly and weakly. This generally results in hydrogen storage thermodynamic properties that represent an interpolation of the individual constituent elements[17]. Under typical hydrogen storage pressure/temperature swing constraints, intermetallic hydrides generally have usable capacities less than 2 wt% hydrogen[17,22], although some high entropy alloys exhibit saturation capacities exceeding 3% and hydrogen-to-metal ratios (H/M) exceeding 2[35,36]. Common advantages of intermetallic MHs are rapid and reversible hydrogen charging and discharging rates, high volumetric densities, and their operation at near-ambient temperatures and low pressures[37]. Complex hydrides exhibit significantly higher hydrogen gravimetric uptakes, typically ranging from 4 to 14 wt% hydrogen[38]. However, they are limited by slow kinetics, requiring higher operating temperatures and pressures for effective use[15,37,39]. We determine the usable hydrogen uptake from experimentally measured PCT curves, within a specific operating pressure range and temperature, as shown in Figure S1. A 2-bar pressure limit during the desorption is chosen to facilitate hydrogen flow from the storage tanks to the fuel cell stacks. We restrict the storage pressure to less than 170 bar, which is set mainly to avoid using tanks other than Type I storage tanks. We also obtained the material properties such as density, heat capacity, thermal conductivity and absorption enthalpy from literature (Table S2).

The storage tank designed for the base case scenario includes a metal hydride bed and cooling/heating tubes as shown in Figure S2a. During the hydrogen charging process, the metal hydride generates heat, which must be effectively removed to facilitate continuous hydrogen uptake. Conversely, during the discharging process, sufficient heat must be supplied to maintain the necessary temperature. Coolant or heating steam is circulated through these tubes to facilitate efficient heat transfer, thereby enhancing the charging and discharging kinetics. The number and spacing of the cooling tubes within the tank are calculated using the adiabatic form of the metal hydride acceptability envelope in cylindrical coordinates, a model previously developed by Corgnale et al.[40]. Based on the number of tubes, the internal diameter of the tank, and outer dimensions of the storage tank can be estimated using the "Tankinator" model and "Design Tool"

developed at Pacific Northwest National Laboratories[28,41,42]. To fine-tune the parameters, we integrate all codes into Python, rather than using the previously developed Excel Visual Basic for Application code. To provide a comparison with the base case tank design, we also evaluated an alternative tank configuration as depicted in Figure S2b. In this design, we assumed that an external cooling tube surrounds the metal hydride bed. However, the limited contact surfaces necessitated a smaller tank diameter to ensure adequate heat transfer between the tank and the coolant. Effects of these two tank designs on the system performance are investigated and included in SI Note 1 and Figure S2c and S2d.

Key system-level assumptions in this analysis include first, the temperature dependence of the heat capacity of MH and storage tanks is neglected. Second, the detailed internal mass and heat transfer effects within the storage tanks are not considered. This includes complex interactions between hydrogen gas and the storage medium, such as hydrogen diffusion and leakage, and the thermal conductivity and heat capacity of MHs and storage tanks are assumed to remain constant, independent of hydrogen concentration and temperature. Third, the kinetics of MHs are acknowledged but not included in the TEA analysis. Lastly, heat exchange and insulation between the ambient and the storage system are studied, but their cost is negligible and therefore not included in the TEA analysis.

System-level performance and TEA

Based on the system boundary, operational cycles, material selection and tank design described above, we conduct a critical analysis of the system-level performance of the MH hydrogen storage system, focusing on energy density, footprint, and cost performance. The energy density is calculated by dividing the energy released from each storage tank by the tank's total volume. Using the size of each tank, the total number of tanks and separation distance between tanks and the overall storage system, we estimate the required footprint for the entire storage system. We then analyze the LCOS of the MH hydrogen storage system by normalizing the capital investment and operational costs over the system's operating lifetime against the output power and comparing it to compressed gas hydrogen storage systems. The power and energy required to size and compute the capital and operation costs of various equipment are determined using an energy balance method across the different operation stages[30,43]. Additional costs, such as maintenance, labor, land

price, and direct and indirect cost, are also considered. More detailed cost factors are provided in Table S5 with detailed TEA modeling available in SI Note 2. The effects of storage tank size on LCOS, various methods of determining labor costs, and insulation considerations are presented in Figure S3, S4 and S5, respectively. In addition to our base case scenario, we also investigate the effects of charging rate, number of cycles, and power scales on LCOS, which will be discussed in detail in the results section. The performance of MH-based hydrogen storage systems is compared to conventional compressed gas hydrogen storage at 170 bar and 350 bar. In contrast, onboard transportation applications use 700 bar pressure to maximize storage capacity, which requires expensive high-pressure storage tanks that have yet to be demonstrated at large storage capacities[44]. Therefore, such high-pressure storage is not considered for large stationary applications and is not analyzed in this study.

Results and discussion

Performance of MH-based hydrogen storage

Figure 2 presents the system-level volumetric energy density and levelized cost of storage (LCOS) for selected MHs compared to physical compressed gas hydrogen storage. Volumetric energy density is defined as the amount of energy stored within the volume of a storage tank, with the tank's detailed design and calculations also provided in SI Note 1, Table S3 and Figure S2. The LCOS represents the annualized equivalent of fixed capital investment and operational costs – including energy, labor maintenance and other costs related to the stored hydrogen per year, excluding the electrolysis and fuel cells. Calulations for these parameters are presented in SI Note 2. Figure 2a illustrates the performance of MHs under various operating temperatures and pressures (denoted by different symbols and colors, respectively) in the base case scenario. All MHs demonstrate a higher volumetric energy density than compressed gas, ranging from 1.2 to 2.5 times greater than 350 bar compressed gas, and 2.24 to 4.74 times greater than 170 bar compressed gas storage system. This clearly shows the advantage of requiring smaller storage footprint. For the LCOS, all intermetallic MHs exhibit a higher LCOS (ranging from \$0.482/kWh to \$1.27/kWh depending on the operating conditions) compared to compressed gas systems. Among the intermetallic MHs, $TiFe_{0.85}Mn_{0.05}$ at 328 K and 25 bar has the lowest cost (\$0.453/kWh), attributed to its combination of relatively high gravimetric capacity (1.84%), low absorption

pressure (25 bar), moderate operating temperature (328 K) and mild absorption enthalpy (32.5 kJ/mol)[32]. In contrast, the complex MH system ($2Mg(NH_2)_2$-2.1LiH-0.1KH), under its optimal operating conditions, has a slightly lower LCOS ($0.383/kWh to $0.395/kWh) than 350 bar compressed gas ($0.397/kWh), primarily due to their higher hydrogen uptake, which reduces the amount of MH required. The cost of MHs is a major component of the system cost, and a reduction in MH price offsets the increased cost associated with more demanding operating conditions (higher temperature, higher pressure and larger heat management needs) for complex MHs. It is important to note that the system cost performance is highly sensitive to the actual cost of MHs, which we have assumed to be $20/kg as the base case for all MHs.

Figure 2b shows the results for the second scenario, where an additional 5wt% gas-phase hydrogen is stored in each tank to initiate fuel cells and the waste heat from fuel cells (80°C) is used to supply the required heat during desorption for the intermetallic MHs. The storage costs are reduced, bringing them closer to the LCOS of 350 bar compressed gas, and improving their economic competitiveness. However, this approach involves a tradeoff, as the increased storage of gas-phase hydrogen results in a decrease in system volumetric energy density. Among the systems, $TiFe_{0.85}Mn_{0.05}$ at 328 K and 25 bar achieves the lowest LCOS ($0.406/kWh) with a good balance of volumetric energy density (0.646 kWh/L).

Figure 3a provides a comprehensive analysis of the LCOS cost breakdown for MHs and compressed gas systems. The price of MHs is the main component of the capital cost for MH-based hydrogen storage, whereas compressed gas incurs higher costs due to the use of Type 3 tanks for 350 bar compressed gas. $2Mg(NH_2)_2$-2.1LiH-0.1KH requires lower investment in the storage material due to its third times higher hydrogen uptake compared to intermetallic MHs. In the 5 wt% gas and waste heat scenario, similar trends are observed as in the base case, with a marginal impact on overall costs due to the inclusion of external heat, which reduces the capital and operational costs of the heater. Since the capital investments in equipment are related to the power they are designed to provide, their costs become more economical when slower charging is allowed, as presented in Figure 3b. This effect is more pronounced in complex MH case (purple line in Figure 3b), where cost for heat management constitutes a large portion of system costs. The required storage space for MHs decreases notably with longer charging times (Figure 3c). This is because the required number of coolant tubes inside each tank decreases with slower charging, leading to a smaller tank size and an overall reduction in storage area. MH systems show a much smaller

required storage area compared to the compressed gas system due to their high volumetric energy density. While onshore plants may have sufficient land for large storage facilities, the price of materials becomes an important factor; in contrast, for offshore applications or backup power in high-land-cost urban areas, space is constrained, making compact storage more desirable[13]. Additionally, MHs require fewer storage tanks to provide the same power compared to compressed gas, making installation, maintenance and infrastructure costs lower. Their smaller footprint also enhances scalability and flexibility, making them ideal for diverse applications while minimizing environment impact. The effects of annual operating cycles on LCOS are shown in Figure 3d. Increasing the frequency of cycles reduces the capital cost per cycle (or per energy produced), as the system is utilized more frequently, leading to a decrease in the marginal cost of capital—an effect that enhances economic efficiency. With fewer cycles, the storage time between charging and discharging is extended; for instance, one cycle per year implies storing hydrogen for 357 days after charging, which characterizes long duration energy storage. In contrast, a higher number of cycles means that hydrogen is stored for a shorter period before being discharged for energy generation. Compared to 350-bar compressed hydrogen gas, intermetallic $TiFe_{0.85}Mn_{0.05}$ has a higher capital cost, resulting in a higher LCOS at low cycle frequencies. However, as the number of cycles increases, the economies of scale come into play, leading to a sharper decrease in LCOS for $TiFe_{0.85}Mn_{0.05}$, narrowing the difference with 350-bar gas. $2Mg(NH_2)_2$-2.1LiH-0.1KH, on the other hand, have lower capital costs due to the reduced amount of MH required (Figure S9), but they incur higher operational energy costs. While the lower capital costs keep the LCOS for complex MH low at a small number of cycles, the impact of capital cost savings diminishes as the number of cycles increases. In contrast, the higher operational costs do not benefit from increased cycling. As a result, with further cycling, the operational costs eventually outweigh the capital savings, potentially causing the LCOS for $2Mg(NH_2)_2$-2.1LiH-0.1KH to surpass that of the other two methods. In summary, intermetallic MHs with higher capital costs due to the larger amount of MH used are more favorable when the system is used frequently. In contrast, complex MH $2Mg(NH_2)_2$-2.1LiH-0.1KH with lower MH costs are more competitive when the system is used less frequently.

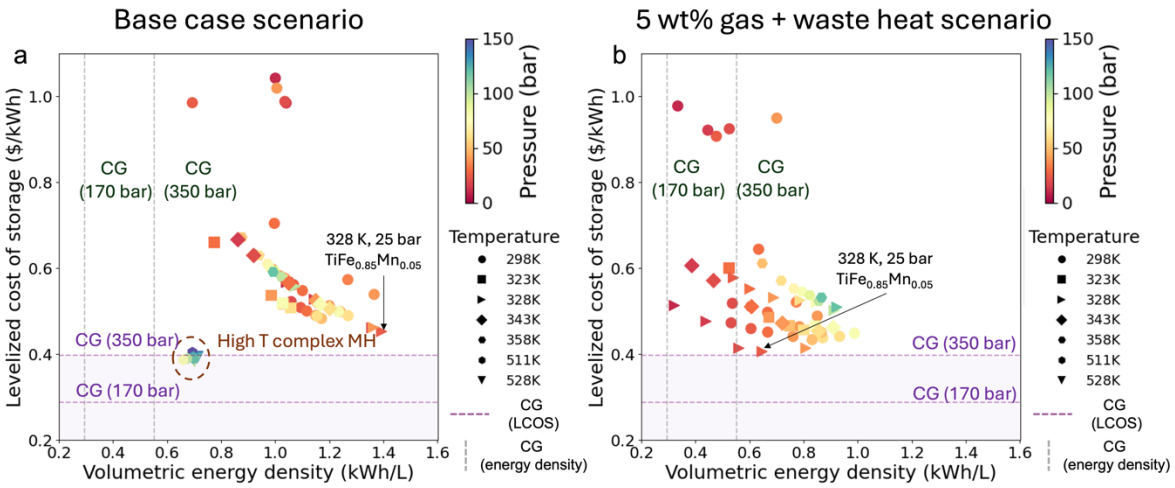

Figure 2. Performance comparison between MHs and compressed gas hydrogen storage methods. (a) Base case scenario: LCOS and volumetric energy density of MHs across various operating temperatures and pressures, benchmarked against compressed gas storage. (b) Alternative scenario: LCOS and volumetric energy density for intermetallic MHs storing 5 wt% of hydrogen in the gas phase to initialize the fuel cell, with subsequent utilization of waste heat from fuel cells to drive the discharge process. All cases assume 12 complete discharges per year.

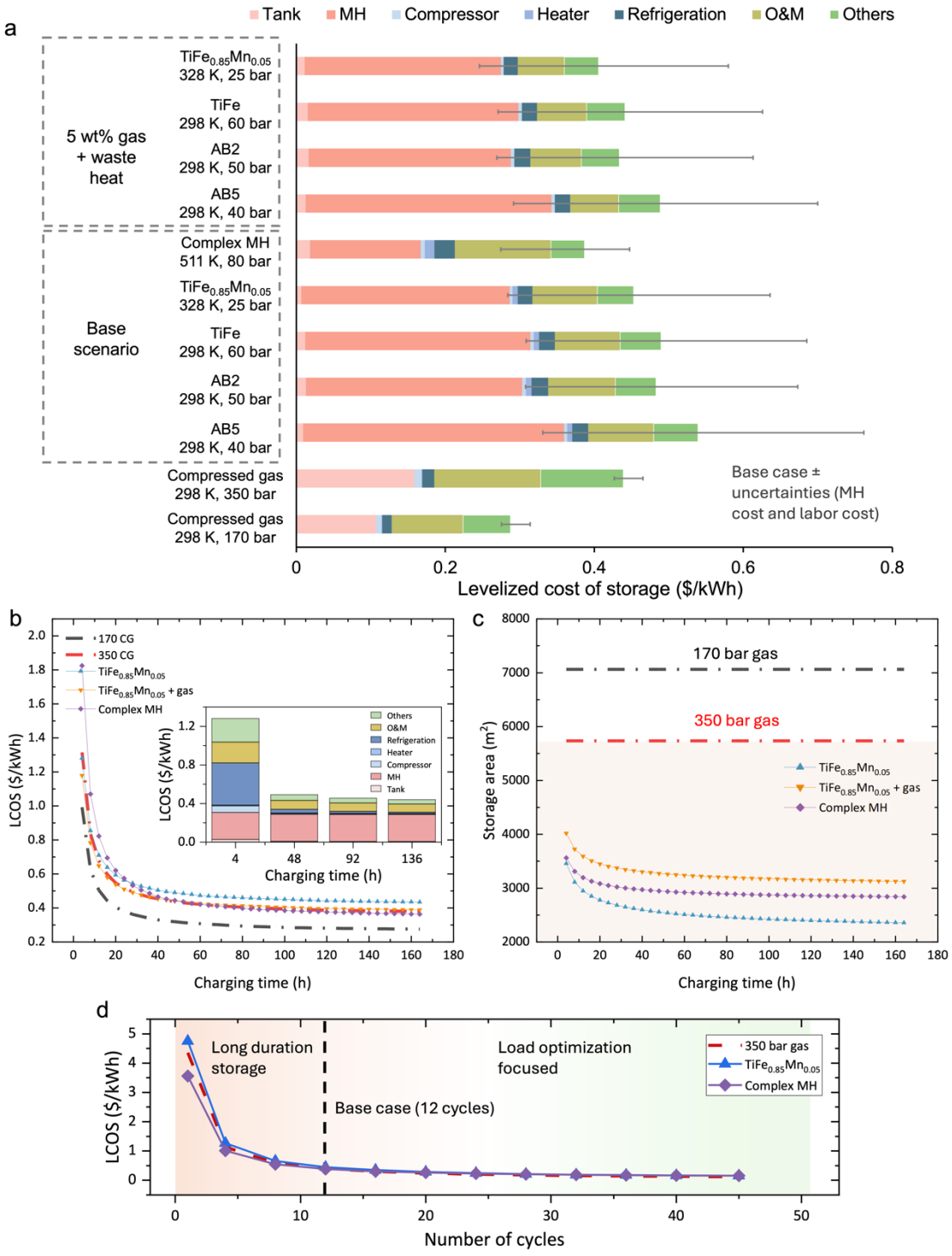

Figure 3. Cost breakdown of MHs and comparison with compressed gas hydrogen storage methods. (a). LCOS breakdown for selected MHs hydrogen storage in two scenarios compared with compressed gas hydrogen storage. 'Others' represents the direct and indirect costs such as

installation cost, piping, contingency, legal and insurance, and site preparation. 'O&M' refers to operation and maintenance. Error bar accounts for variations in labor cost ($25/hour to $60/hour) and MH cost ($10/kg to $30/kg). (b) The effects of charging time on the LCOS for MHs and compressed gas. The inset graph shows the effects of charging time on the LCOS breakdown for the $TiFe_{0.85}Mn_{0.05}$ base case scenario. (c) Effects of charging time on the required storage space for MHs and compressed gas. (d) Effect of annual operating cycles on the LCOS for representative MHs and 350-bar compressed hydrogen gas. The color gradient in the background highlights different application focuses: orange represents long-duration, backup-focused applications, while blue represents load optimization-focused applications requiring short-term storage between charging and discharging. The black dashed vertical line indicates 12 annual cycles, corresponding to the base case scenario.

Effects of material properties and future development targets

To better understand the effects of individual material properties on the overall LCOS, we conducted a sensitivity analysis using a hypothetical MH system. We assume this MH has a hydrogen uptake of 1.5 wt% at 333 K and 60 bar pressure, and a release efficiency of 90% (resulting in a usable hydrogen release of 1.35 wt%). The enthalpy of hydrogen absorption is assumed to be 30 kJ/mol. By varying each material property independently, while holding the others constant, we calculate the resulting LCOS, as shown in Figure 4a to 4f. For instance, when the operating pressure is varied from 20 bar to 100 bar, while maintaining the constant uptake and power, the LCOS increases from 0.54 $/kWh to 0.58 $/kWh (Figure 4a), corresponding to an incremental rate of 0.0005$/kWh per bar. This increase is primarily due to the higher costs associated with the storage tank and the expenses of the compressor. Conversely, an increase in hydrogen uptake decreases the LCOS, as it reduces the required amount of MH (Figure 4b) and therefore costs in both the storage tank and related equipment. Packing porosity refers to the voids between the MH particles when they are packed together. As shown in Figure 4c, the impact of packing porosity on LCOS is minimal, as it only slightly raises the storage tank cost, which represents a small fraction of the overall system cost. Economically, loosely packed MHs are feasible as long as space constraints are not a significant concern, providing additional room for MH expansion during hydrogen absorption.

It is important to acknowledge that while this analysis isolates each parameter, many material properties are correlated. For example, from the van't Hoff equation, the absorption enthalpy is a function of the equilibrium pressure and operating temperature, and materials with higher uptake typically exhibit higher absorption enthalpy due to stronger metal-hydrogen bonding interactions[45]. This analysis highlights the significance of each material property on the LCOS. For example, a 0.4 wt% increase in hydrogen uptake can reduce the LCOS by 0.09$/kWh. Even if achieving this uptake requires higher operating temperatures or enthalpy, the overall cost reduction may still justify the trade-off, as savings from increased uptake outweigh the additional costs. However, a more detailed analysis of the relationship between uptake and enthalpy is needed in future work, as understanding the rate at which enthalpy changes with uptake is critical for determining cost trade-offs. Finally, material degradation also plays a critical role in LCOS, with better cyclability and reduced degradation being crucial for economic feasibility (Figure 4e).

Figure 4g presents the potential for reducing the LCOS for the current MHs. The roadmap details the storage system costs using $TiFe_{0.85}Mn_{0.05}$ under conditions of 328 K and 25 bar as the base case. In this scenario, the cost is around 1.2 times higher than that of 350 bar compressed gas, and 1.6 times higher than 170 bar compressed gas. Cost reduction can be achieved through advancements in material properties and engineering design, such as leveraging waste heat for enhanced thermal management, improving material thermal conductivity, increasing hydrogen uptake and reducing the cost of MHs. In the near term, known improvements in material manufacturing and the use of low-cost raw material are expected to reduce MH costs. As noted in Figure 4g, by decreasing the MH price to $10/kg, MH-based hydrogen storage could outperform 170 bar compressed gas in LCOS.

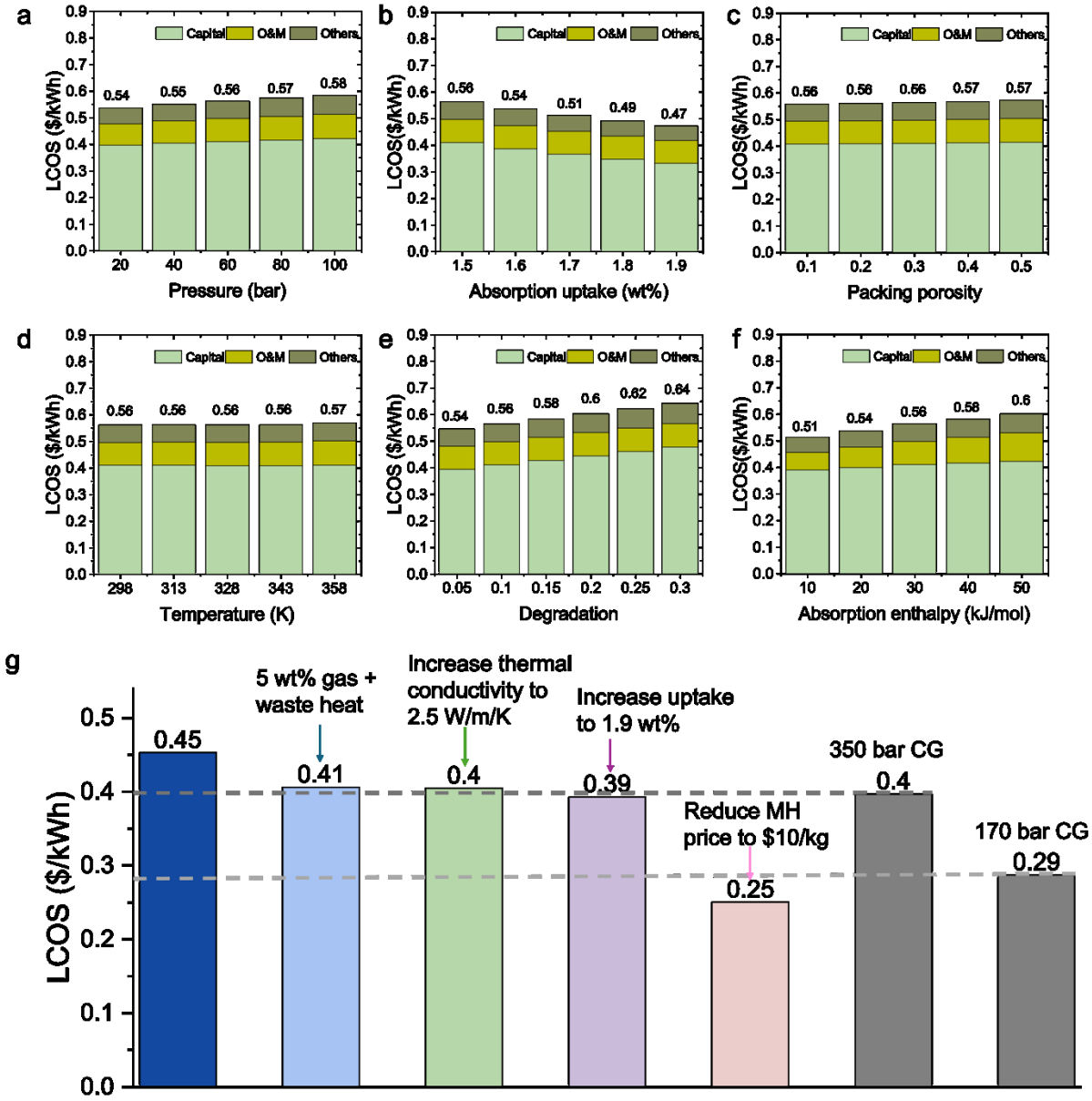

Figure 4. Effects of material properties on LCOS and material targets. (a-f) The panels illustrate the effects of varying individual material properties on the LCOS and the corresponding cost breakdown. Each panel examines the impact of changing one specific property at a time. (g) A roadmap for reducing LCOS of an H_2 storage system, starting from the base case of $TiFe_{0.85}Mn_{0.05}$ under 328 K and 25 bar. The diagram highlights the reduction in LCOS achievable through various methods and compares these results with compressed gas storage systems.

System scalability

Hydrogen can be stored in a wide range of quantities, providing exceptional scalability as an energy carrier for energy storage. This scalability makes hydrogen a particularly promising solution for power supply, capable for meeting the needs of both small- and large-scale applications. Figures 5a and 5b show the total hydrogen amount, and the corresponding MH requirements as a function of power supply duration and power size. A system with a power size of 5 MW or below is sufficient for supporting a small data center, whereas a power size between 5 MW and 20 MW would be suitable for a medium-sized data center. The power duration refers to the time that the system can continuously supply energy; in our base case, we assumed 96 hours. As power duration and size increases, more hydrogen needs to be stored, thereby necessitating a greater amount of MH. However, as power size and duration further increase, MH-based storage systems face significant limitations due to the escalating material requirements. For example, providing 20 MW of power for 100 hours would require nearly 8,000 tons of intermetallic $TiFe_{0.85}Mn_{0.05}$ MH , raising concerns about the feasibility of manufacturing such a large quantity. In contrast, complex MH $2Mg(NH_2)_2$-2.1LiH-0.1KH, with its higher hydrogen uptake, reduce the required amount to be around 3,000 tons, making them more practical in material production and large-scale backup power applications. For each power scale, we calculated the LCOS of $TiFe_{0.85}Mn_{0.05}$ at 328 K and 25 bar, as shown in Figure 5c. The LCOS remains relatively high for smaller power sizes and shorter durations but decreases as both parameters increase. This reduction in LCOS with larger power scales is primarily due to the realization of economies of scale, where the capital cost of equipment is better distributed across the larger power output. Additionally, we calculated the difference in LCOS between the $TiFe_{0.85}Mn_{0.05}$ and 350-bar compressed gas as presented in Figure 5d. Interesting, the trend in LCOS difference is not linear; for smaller power sizes and shorter durations, the difference is significant, indicating that the LCOS of MHs is much higher than that of 350-bar compressed gas. However, MHs are more advantageous in medium to long durations (50 to 100 hours) and power sizes between 3.75 MW and 16.25 MW (except for the 8.75 MW), where the LCOS difference is around $0.05/kWh. The reason the difference in LCOS is not linear because, for different power scales, we assume equal charging and discharging times (power durations). With the same charging time, increasing the power scale requires a higher charging rate, which raises the system's LCOS. However, the economies of scale work to reduce LCOS as the power scale increases. The combined effects of

these two factors influence the overall LCOS. Since the impact of charging rate is non-linear and more pronounced in MHs compared to compressed gas, the LCOS difference between the two methods increases at certain points. Overall, these results suggest that while MH-based hydrogen storage systems like $TiFe_{0.85}Mn_{0.05}$ offer potential benefits, especially for medium to long-duration energy storage. However they face challenges for large-scale power applications over extended durations due to the significant and unprecedented manufacturing volumes of hydrides needed to satisfy market demands[46,47].

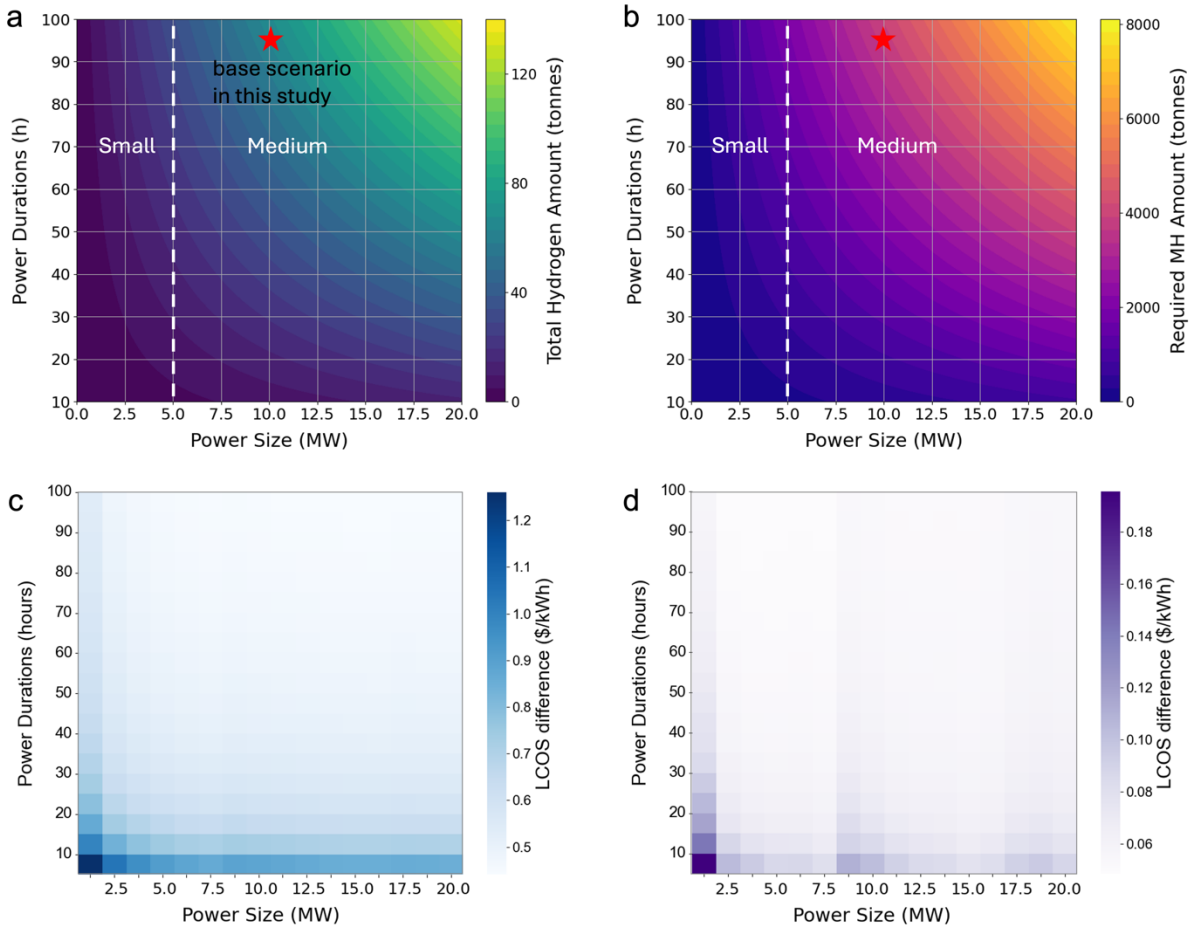

Figure 5. Scalability of the hydrogen storage system. (a-b) Total stored hydrogen and required MHs amounts as functions of power durations and power size, respectively. (c) LCOS for $TiFe_{0.85}Mn_{0.05}$ at 328 K and 25 bar across various power scales. (d) LCOS difference between $TiFe_{0.85}Mn_{0.05}$ at 328 K and 25 bar and a 350-bar compressed gas system.

Uncertainties and future direction

In this study, we conducted a system-level cost analysis of MH-based hydrogen storage for backup power applications and benchmarked it against the compressed gas method. Our results suggest that MHs offer a compelling combination of high volumetric energy density and low operating pressures compared to compressed gas hydrogen storage. These advantages not only reduce the required footprint but also reduce the safety concerns and system complexity. Intermetallic MHs could potentially achieve cost parity with 350 compressed gas in terms of LCOS when integrated with external heat sources, such as waste heat from fuel cells. Additionally, allowing for a slower charge rate could further decrease the LCOS and reduce the system footprint for MHs. Among all the expenditures, the material cost of MHs is the most significant capital expense in the storage system. Therefore, future advancements in MH technology - such as developing MHs with higher uptakes, or using less expensive raw materials and enhanced manufacturing techniques- could further reduce costs, making MHs even more competitive with compressed gas method. Beyond evaluating the overall cost performance of this emerging technology, our study also identified key limitations and critical areas for future research, as outlined below.

Our analysis is grounded in experimental measurements of PCT curves for hydrogen absorption and desorption in MHs. Accurate measurements of hydrogen uptake and corresponding PCT curves are important for assessing hydrogen capacity and heat enthalpy. However, variations in hydrogen uptake variations can occur even with identical compositions due to factors such as synthesis variations, impurities, phase separation and insufficient activation. Furthermore, scaling up hydrogen storage introduces additional variations, as MHs synthesized on an industrial scale may exhibit different hydrogen absorption properties compared to those synthesized in the laboratory[48].

For long duration hydrogen storage, which requires large amount of MH, standardizing industrial-scale material synthesis and accurately quantifying hydrogen absorption performance are critical areas for future research. In addition to experimental data, accurate simulation results can further explore the potential of MHs in hydrogen storage. Unlike the extensive molecular simulations and machine learning investigations of hydrogen uptake in physisorption-based metal organic frameworks (MOFs)[49–52], the complexity of hydrogen absorption by MH, encompassing physisorption, chemisorption, diffusion, and phase transformations, is computationally expensive

to simulate. Although ML has been used to predict hydrogen diffusion in MHs[53], hydride formation enthalpy[54], thermodynamic stability[35] and phase diagrams[56], future research should target using standardized experimental methods or computational simulations to generate sufficient data for MH-based hydrogen storage. These data could then be employed to interpolate hydrogen absorption performance using ML models.

The primary capital cost for MH-based hydrogen storage is attributed to the price of MHs. In this study, we assumed a uniform price of $20/kg for all MHs tested, with error margin ranging from $10/kg to $30/kg. However, this is a rough estimate, as different MHs generally have varying prices. For example, AB and AB_2-type hydrides can be cheaper than AB_5 hydrides based on the cost of rare-earth elements. The price of MHs comprises two major components: raw material costs and manufacturing costs. The raw material cost depends on the elements used; For instance, Mn, Al, and Fe, Mg, Cr and Ti are relatively inexpensive, while Zr, Mo, W, Co and V are more costly[57,58]. The manufacturing cost of MHs, which is highly dependent on synthesis methods and production scale, remains underexplored[45]. A more detailed analysis of MH prices is crucial for future research to provide a more accurate commercial potential assessment for MHs in hydrogen storage.

Metal hydride reactions require efficient heat removal during the charging and heat supply during discharging. Achieving this poses challenges due to the poor heat transfer characteristics of metal hydride powders, which can potentially reduce the reaction rate. To mitigate this limitation, we used a tank design to enhance heat transfer. In each tank, we calculated the required number of coolant tubes to achieve the desired charging and discharging rate. Additionally, compaction of powders into pellets or plates, supplemented with expanded natural graphite (ENG), is a common method to improve thermal conductivity and packing density[59] As shown in SI Note 4, adding ENG can initially reduce the levelized cost of storage for $LaNi_5$ MH. However, further increases in ENG lead to higher costs due to the resulting decrease in volumetric energy density. Other methods, such as tubes fins and aluminum foam have also been employed[60]. The impact of these methods on the thermal properties of MHs and their cost performance requires further investigation. Moreover, we used the energy balance method to evaluate the total amount of heat that must be supplied during the discharging, assuming the use of high temperature steam for heat transfer. However, identifying the most efficient method for large-scale industrial heat transfer remains a challenge to widespread application of MHs. In addition to the heat supply analyzed in this study,

other potential sources for providing heat during discharge include combustion of a portion of the hydrogen released from the storage material. As shown in SI Note 7, this approach would require storing at least 20% more hydrogen to account for combustion needs. Moreover, the cold start challenge must be addressed for this strategy to be effective. Although the overall LCOS was not calculated for this scenario, it is clear that it would be higher than our base case, as a portion of the stored hydrogen would not be available for electricity generation via fuel cells. However, this approach could enable a self-sustained system without the need for external fuel or electricity. Another theoretical solution involves storing the heat generated during the charging process (an exothermic reaction) and reusing it during discharge. While promising, the technical feasibility of this approach for large-scale hydrogen storage, especially for backup power applications with long cycle durations, remains uncertain. The use of phase-change materials (PCM) has been studied for storing heat[60,61], but the practicality of this approach, considering the massive amount of PCM required and the associated energy costs, requires further investigation.

Additionally, the cyclability and degradation of MHs play vital roles in their competitiveness for hydrogen storage applications. In this study, we estimated a requirement of 12 cycles per year, totaling approximately 360 cycles over a 30-year lifespan. We postulated a 10% loss of storage capacity for all MHs evaluated, based on limited information available in the literature (SI Note 3). This degradation rate, however, is likely to vary across different MH materials. Accurate experimental testing of MH cyclability and degradation is important for evaluating system-level cost performance.

Kinetics is another critical property that determines the practical application of MHs for hydrogen storage. Intermetallic MHs tends to exhibit favorable thermodynamics and fast kinetics, whereas lightweight hydrides and complex hydrides, which have high storage capacities, often have suboptimal thermodynamics and slow kinetics[62]. For long-duration hydrogen storage, rapid hydrogen absorption is less critical compared to transportation applications, where refueling needs to occur in minutes. The primary goal for stationary hydrogen storage is to safely store hydrogen for extended periods while maximizing volumetric energy density. For MHs with sluggish kinetics, multiple storage tanks can be charged and discharged simultaneously to meet the required hydrogen input rate for fuel cells, allowing sufficient time for each tank to complete its cycle. Thus, a detailed kinetic analysis was not included in this study and but should be considered in future investigations of system-level storage costs. Extensive research has been conducted to improve

absorption and desorption kinetics through alloying, nano-sizing, and catalysis at the laboratory scale[62–64]. However, understanding how to scale up these promising MHs and their effects on cost performance is important for future research.

Finally, for PEM electrolyzers, the H_2 outlet pressure is ~30 bar, which is sufficient to avoid the need for a compressor in intermetallic MH-based hydrogen storage systems. The required inlet pressure for a PEM fuel cell ranges from 2-5 bar, an achievable pressure level during desorption from MH storage[37,65]. In this study, a desorption pressure limit of 2 bar was employed. However, large-scale power storage systems may encounter significant pressure drops during hydrogen flow through pipelines, adversely affecting system performance and increasing the LCOS. As detailed in SI Note 5, increasing this limit to 5 bar to account for potential pressure drops results in a rise in LCOS. The exact value of pressure drops and potential hydrogen loss during dispensing depends on the coupling of the MH-H_2 storage system with the plant design and specific dispensing distance. These factors were not included in the current model and deserve further investigation to optimize hydrogen storage system design and operation.

Conclusion

In this study, we introduce novel process designs for metal hydride-based hydrogen storage systems for backup power applications. We calculate their system energy density, footprint and LCOS, benchmarking them against compressed gas hydrogen storage, and set targets for materials development.

We employ a storage tank design with internal cooling tubes, optimized using the "acceptability envelope" method. Coolant or heating steam is circulated through these tubes to facilitate efficient heat transfer during charging and discharging processes. After charging, the storage tank is allowed to cool down to room temperature. Before discharging, the tank is reheated to release the hydrogen at the required operating temperature. We then calculate the capital and operational costs of various equipment using an energy balance method, accounting for the power and energy required to size the equipment across the different operational stages.

For a base case scenario with 96-hour charging, 10 MW discharge for 96 hours, and 12 operating cycles per year, intermetallic MHs exhibit higher LCOS compared to physical based hydrogen

storage but offer significantly higher energy density and a substantial advantage in land footprint, requiring up to 65% less space than 170 bar compressed gas storage. Storing 5% of gas and utilizing waste heat from the fuel cell further reduce the LCOS of intermetallic MHs. However, this approach involves a trade-off, as the increased storage of gas-phase hydrogen results in a decrease in system volumetric energy density. Among the intermetallic materials analyzed, $TiFe_{0.85}Mn_{0.05}$ at 328 K and 25 bar achieves the lowest LCOS ($0.406/kWh) with a good balance of volumetric energy density (0.646 kWh/L). Complex MH 2Mg(NH2)2-2.1LiH-0.1KH achieves a lower LCOS than 350 bar compressed gas, primarily due to high hydrogen uptake and reduced capital cost, which offset the increased operational costs.

Extending the charging time reduces the LCOS across all systems by lowering the power requirements for key equipment. $2Mg(NH_2)_2$-2.1LiH-0.1KH shows the most significant reduction in LCOS due to their higher reliance on heat removal and cooling. Additionally, slower charging further reduces the required footprint for MHs, as fewer cooling tubes are needed in each tank, making MHs more competitive for applications with limited space. Meanwhile, increasing the frequency of annual operating cycles reduces the LCOS for all systems. However, intermetallic MHs experience a more substantial reduction due to their higher capital costs, which benefit from more frequent use. In contrast, complex MH $2Mg(NH_2)_2$-2.1LiH-0.1KH with lower capital costs are more competitive when the system is used less frequently, making them suitable for long-duration energy storage.

To further enhance the economic competitiveness of MHs, future research should focus on optimizing thermal management, increasing hydrogen uptake, and reducing MH production costs. These advancements are crucial for realizing the full potential of MH-based hydrogen storage systems. Our analysis of various power scales and durations indicates that MH-based hydrogen storage systems offer significant potential for medium power and medium to long-duration energy storage. However, large-scale power applications over extended durations remain challenging due to the substantial manufacturing volumes of MH required to meet market demands (although this problem is not unique to MHs).

Conflicts of interest

There are no conflicts to declare.

Acknowledgements

The authors gratefully acknowledge support from the U.S. Department of Energy (DOE) under Contract No. DE-AC02-05CH11231 with the Lawrence Berkeley National Laboratory. Sandia National Laboratories is a multi-mission laboratory managed and operated by National Technology & Engineering Solutions of Sandia, LLC (NTESS), a wholly owned subsidiary of Honeywell International Inc., for the U.S. DOE's National Nuclear Security Administration (DOE/NNSA) under contract DE-NA0003525. This written work is authored by an employee of NTESS. The employee, not NTESS, owns the right, title and interest in and to the written work and is responsible for its contents. Any subjective views or opinions that might be expressed in the written work do not necessarily represent the views of the U.S. Government. The publisher acknowledges that the U.S. Government retains a non-exclusive, paid-up, irrevocable, world-wide license to publish or reproduce the published form of this written work or allow others to do so, for U.S. Government purposes. The DOE will provide public access to results of federally sponsored research in accordance with the DOE Public Access Plan. The authors gratefully acknowledge research support from the U.S. DOE, Office of Energy Efficiency and Renewable Energy, Fuel Cell Technologies Office through the Hydrogen Storage Materials Advanced Research Consortium (HyMARC**).** The authors thank Drs. Ned Stetson, Zeric Hulvey, and Marika Wieliczko for their support and guidance.

References

1. Department of Energy Report. https://www.energy.gov/ne/articles/department-energy-report-explores-us-advanced-small-modular-reactors-boost-grid (2018).
2. Weather-related Power Outages Rising. https://www.climatecentral.org/climate-matters/weather-related-power-outages-rising.
3. Eric Masanet, Arman Shehabi, Nuoa Lei, S. S. and J. K. Recalibrating global data center energy-use estimates. *Science (80-.).* **367**, 984–986 (2020).
4. Bawaneh, K., Nezami, F. G., Rasheduzzaman, M. & Deken, B. Energy consumption analysis and characterization of healthcare facilities in the United States. *Energies* **12**, (2019).
5. S. Bouckaert, A.F. Pales, C. McGlade, U. Remme, B. W. Net Zero by 2050. A Roadmap for the Global Energy Sector. https://www.iea.org/reports/net-zero-by-2050. *Int. Energy Agency* (2021).
6. Kebede, A. A., Kalogiannis, T., Van Mierlo, J. & Berecibar, M. A comprehensive review of stationary energy storage devices for large scale renewable energy sources grid integration. *Renew. Sustain. Energy Rev.* **159**, 112213 (2022).
7. Kurtz, J. *et al.* Hydrogen fuel cell performance as telecommunications backup power in the United States. 41 (2015).
8. Ghimire, R., Niroula, S., Pandey, B., Subedi, A. & Thapa, B. S. Techno-economic assessment of fuel cell-based power backup system as an alternative to diesel generators in Nepal: A case study for hospital applications. *Int. J. Hydrogen Energy* **56**, 289–301 (2024).
9. Saur, G. Prototype Integrated Hydrogen Fuel Cell Powered Data Center: Cooperative Research and Development Final Report, CRADA Number CRD-17-00709. (2022).
10. Kurtz, J. *et al.* Analysis of hydrogen infrastructure for the feasibility, economics, and sustainability of a fuel cell powered data center. *Sustain. Energy Technol. Assessments* **58**, 103357 (2023).
11. Saur, G., Arjona, V., Clutterbuck, A. & Parker, E. Hydrogen and Fuel Cells for Data

Center Applications Project Meeting: Workshop Report. (2019).

12. Curtin, S. & Gangi, J. State of states: fuel cells in America 2017. *U.S. Dep. Energy* 1–76 (2018).

13. Adams, M. J., Wadge, M. D., Sheppard, D., Stuart, A. & Grant, D. M. Review on onshore and offshore large-scale seasonal hydrogen storage for electricity generation: Focusing on improving compression, storage, and roundtrip efficiency. *Int. J. Hydrogen Energy* **73**, 95–111 (2024).

14. Hirscher, M. *et al.* Materials for hydrogen-based energy storage – past, recent progress and future outlook. *J. Alloys Compd.* **827**, (2020).

15. Allendorf, M. D. *et al.* Challenges to developing materials for the transport and storage of hydrogen. *Nat. Chem.* **14**, 1214–1223 (2022).

16. Amos, W. A. Costs of storing and transporting hydrogen. *NREL 1998* **16**, 343–351 (1991).

17. Andersson, J. & Grönkvist, S. Large-scale storage of hydrogen. *Int. J. Hydrogen Energy* **44**, 11901–11919 (2019).

18. Takagi, S. & Orimo, S. I. Recent progress in hydrogen-rich materials from the perspective of bonding flexibility of hydrogen. *Scr. Mater.* **109**, 1–5 (2015).

19. Mohtadi, R. & Orimo, S. I. The renaissance of hydrides as energy materials. *Nat. Rev. Mater.* **2**, 1–16 (2016).

20. Bellosta von Colbe, J. *et al.* Application of hydrides in hydrogen storage and compression: Achievements, outlook and perspectives. *Int. J. Hydrogen Energy* **44**, 7780–7808 (2019).

21. G.Alefeld, J. V. *Hydrogen in Metals I*. (Springer Berlin, Heidelberg, 1978). doi:https://doi.org/10.1007/3-540-08705-2.

22. Modi, P. & Aguey-Zinsou, K. F. Room Temperature Metal Hydrides for Stationary and Heat Storage Applications: A Review. *Front. Energy Res.* **9**, 1–25 (2021).

23. Danebergs, J. & Deledda, S. Can hydrogen storage in metal hydrides be economically competitive with compressed and liquid hydrogen storage? A techno-economical perspective for the maritime sector. *Int. J. Hydrogen Energy* (2023) doi:10.1016/j.ijhydene.2023.08.313.

24. Mongird, K. *et al.* 2020 Grid Energy Storage Technology Cost and Performance Assessment. *Energy Storage Gd. Chall. Cost Perform. Assess. 2020* 1–20 (2020).

25. Allendorf, M. D., Horton, R., Stavila, V. & Witman, M. Assessment of tank designs for hydrogen storage on heavy duty vehicles using metal hydrides. *Sandia Rep. SAND2023-05851* (2023).

26. Amica, G., Arneodo Larochette, P. & Gennari, F. C. Light metal hydride-based hydrogen storage system: Economic assessment in Argentina. *Int. J. Hydrogen Energy* **45**, 18789–18801 (2020).

27. Allendorf, M. D., Klebanoff, L., Stavila, V. & Witman, M. Assessment of Materials-Based Options for On-Board Hydrogen Storage for Rail Applications. *Sandia Rep. SAND2023-13180* (2023).

28. Brooks, K. *et al.* PNNL Development and Analysis of Material-Based Hydrogen Storage Systems for the Hydrogen Storage Engineering Center of Excellence. (2016).

29. Standard for Emergency and Standby Power Systems (National Fire Protection Association, 2022). *https://www.nfpa.org/codes-and-standards/ all-codes-and-standards/list-of-codes-and-standards/detail?code=110.*

30. Peng, P. *et al.* Cost and potential of metal–organic frameworks for hydrogen back-up power supply. *Nat. Energy* **7**, 448–458 (2022).

31. Cetinkaya, S. A., Disli, T., Soyturk, G., Kizilkan, O. & Colpan, C. O. A Review on Thermal Coupling of Metal Hydride Storage Tanks with Fuel Cells and Electrolyzers. *Energies* **16**, (2023).

32. Dematteis, E. M. *et al.* Fundamental hydrogen storage properties of TiFe-alloy with partial substitution of Fe by Ti and Mn. *J. Alloys Compd.* **874**, 159925 (2021).

33. Voskuilen, T. G., Waters, E. L. & Pourpoint, T. L. A comprehensive approach for alloy selection in metal hydride thermal systems. *Int. J. Hydrogen Energy* **39**, 13240–13254 (2014).

34. Mark D Allendorf *et al.* HyMARC : SNL Activities (ST233). in *2023 Annual Merit Review and Peer Evaluation Meeting* 1–39 (2023).

35. Sahlberg, M., Karlsson, D., Zlotea, C. & Jansson, U. Superior hydrogen storage in high entropy alloys. *Sci. Rep.* **6**, 1–6 (2016).

36. Nygård, M. M. *et al.* Counting electrons - A new approach to tailor the hydrogen sorption properties of high-entropy alloys. *Acta Mater.* **175**, 121–129 (2019).

37. Klopčič, N., Grimmer, I., Winkler, F., Sartory, M. & Trattner, A. A review on metal hydride materials for hydrogen storage. *J. Energy Storage* **72**, (2023).

38. Dematteis, E. M. *et al.* Hydrogen storage in complex hydrides: Past activities and new trends. *Prog. Energy* **4**, (2022).

39. Hwang, H. T. & Varma, A. Hydrogen storage for fuel cell vehicles. *Curr. Opin. Chem. Eng.* **5**, 42–48 (2014).

40. Corgnale, C., Hardy, B. J., Tamburello, D. A., Garrison, S. L. & Anton, D. L. Acceptability envelope for metal hydride-based hydrogen storage systems. *Int. J. Hydrogen Energy* **37**, 2812–2824 (2012).

41. Klymyshyn, N. A., Brooks, K. & Barrett, N. Methods for Estimating Hydrogen Fuel Tank Characteristics. *J. Press. Vessel Technol. Trans. ASME* **146**, 1–10 (2024).

42. Brooks, K. P., Sprik, S. J., Tamburello, D. A. & Thornton, M. J. Design tool for estimating metal hydride storage system characteristics for light-duty hydrogen fuel cell vehicles. *Int. J. Hydrogen Energy* **45**, 24917–24927 (2020).

43. Peng, P. *et al.* Long Duration Energy Storage Using Hydrogen in Metal − Organic Frameworks: Opportunities and Challenges. *ACS Energy Lett.* (2024) doi:10.1021/acsenergylett.4c00894.

44. O'Malley, K. *et al.* Applied hydrogen storage research and development: A perspective from the U.S. Department of Energy. *J. Alloys Compd.* **645**, S419–S422 (2015).

45. Sandrock, G. Panoramic overview of hydrogen storage alloys from a gas reaction point of view. *J. Alloys Compd.* **293**, 877–888 (1999).

46. Jensen, E. H., Dornheim, M. & Sartori, S. Scaling up metal hydrides for real-scale applications: Achievements, challenges and outlook. *Inorganics* **9**, 1–20 (2021).

47. Dematteis, E. M., Berti, N., Cuevas, F., Latroche, M. & Baricco, M. Substitutional effects

in TiFe for hydrogen storage: A comprehensive review. *Mater. Adv.* **2**, 2524–2560 (2021).

48. Barale, J. *et al.* TiFe0.85Mn0.05 alloy produced at industrial level for a hydrogen storage plant. *Int. J. Hydrogen Energy* **47**, 29866–29880 (2022).

49. Ahmed, A. & Siegel, D. J. Predicting hydrogen storage in MOFs via machine learning. *Patterns* **2**, 100291 (2021).

50. Lin, J. *et al.* Machine learning accelerates the investigation of targeted MOFs: Performance prediction, rational design and intelligent synthesis. *Nano Today* **49**, 101802 (2023).

51. Ahmed, A. *et al.* Exceptional hydrogen storage achieved by screening nearly half a million metal-organic frameworks. *Nat. Commun.* **10**, (2019).

52. Bucior, B. J. *et al.* Energy-based descriptors to rapidly predict hydrogen storage in metal-organic frameworks. *Mol. Syst. Des. Eng.* **4**, 162–174 (2019).

53. Lu, G. M., Witman, M., Agarwal, S., Stavila, V. & Trinkle, D. R. Explainable machine learning for hydrogen diffusion in metals and random binary alloys. *Phys. Rev. Mater.* **7**, 1–16 (2023).

54. Batalović, K., Radaković, J., Kuzmanović, B., Medić Ilić, M. & Paskaš Mamula, B. Machine learning-based high-throughput screening of Mg-containing alloys for hydrogen storage and energy conversion applications. *J. Energy Storage* **68**, 1–9 (2023).

55. Witman, M. *et al.* Data-Driven Discovery and Synthesis of High Entropy Alloy Hydrides with Targeted Thermodynamic Stability. *Chem. Mater.* **33**, 4067–4076 (2021).

56. Witman, M. D. *et al.* Phase Diagrams of Alloys and Their Hydrides via On-Lattice Graph Neural Networks and Limited Training Data. *J. Phys. Chem. Lett.* **15**, 1500–1506 (2024).

57. Xinyi Wang, Annalise Kramer, Christopher Glaubensklee, Haoyang He, J. M. S. *Sustainability-based Selection of Materials for Refractory High Entropy Alloys*. *REWAS 2022: Developing Tomorrow's Technical Cycles (Volume I), The Minerals, Metals &Materials Series,* vol. I (2022).

58. Harries, D. N., Paskevicius, M., Sheppard, D. A., Price, T. E. C. & Buckley, C. E. Concentrating solar thermal heat storage using metal hydrides. *Proc. IEEE* **100**, 539–549

(2012).

59. Ye, J., Li, Z., Zhang, L., Wang, S. & Jiang, L. Measurement and the improvement of effective thermal conductivity for a metal hydride bed - a review. *RSC Adv.* **12**, 25722–25743 (2022).

60. Afzal, M., Mane, R. & Sharma, P. Heat transfer techniques in metal hydride hydrogen storage: A review. *Int. J. Hydrogen Energy* **42**, 30661–30682 (2017).

61. Garrier, S. *et al.* A new MgH2 tank concept using a phase-change material to store the heat of reaction. *Int. J. Hydrogen Energy* **38**, 9766–9771 (2013).

62. Mehr, A. S., Phillips, A. D., Brandon, M. P., Pryce, M. T. & Carton, J. G. Recent challenges and development of technical and technoeconomic aspects for hydrogen storage, insights at different scales; A state of art review. *Int. J. Hydrogen Energy* **70**, 786–815 (2024).

63. Webb, C. J. A review of catalyst-enhanced magnesium hydride as a hydrogen storage material. *J. Phys. Chem. Solids* **84**, 96–106 (2015).

64. Schneemann, A. *et al.* Nanostructured Metal Hydrides for Hydrogen Storage. *Chem. Rev.* **118**, 10775–10839 (2018).

65. Ahmadi, N., Dadvand, A., Rezazadeh, S. & Mirzaee, I. Analysis of the operating pressure and GDL geometrical configuration effect on PEM fuel cell performance. *J. Brazilian Soc. Mech. Sci. Eng.* **38**, 2311–2325 (2016).